

Study of Transition Metal Doped ZnO Nanostructures

Dr. V. Lakshmi Priya, Dr. N. Prithivi kumaran
Assistant Professor of Physics
VHNSN College, Virudhunagar

Abstract:- The grain size value of Ni doped ZnO thin films increases with the Ni concentration and it deteriorates the ZnO crystalline quality. The bandgap values of Ni doped ZnO thin films were found to decrease with increase in Ni concentration. The low reflectance and high value of index possessed by ZnO and Ni doped ZnO films are suitable for antireflection coatings. The Optical bandgap values obtained by single oscillator model for ZnO film exactly matches with the Tauc's plot values. The resistivity values of Ni doped ZnO films decrease with increase in Ni doping concentration.

Keywords:- ZnO Nano Structures; Doping; XRD; Refractive Index; Resistivity.

I. INTRODUCTION

Nanocrystalline ZnO is of distinct interest, because of the options for the alteration of various ZnO based nanostructures[1]. In recent years doped ZnO thin films have been the subject of much attention because of their potential for important applications such as a hetero junction device[2], luminescent material[3], gas sensor[4], transparent conductor[5] and dilute magnetic semiconductor[6]. By doping with different metal ions using different techniques can improve the properties of ZnO, particularly the electrical behavior. The isovalent nature of both ZnO and transition metal ions(TM) have made it possible to dope ZnO with Al [7], Ga, Co, Cd[8,9,10], Mg [11] and Ni. Only very few studies has been carried out on ZnO:Ni system due to the phase segregation of ZnO and NiO. This happens due to the large driving force of Ni-O bond as compared to Zn-O bond [12].

Various methods have been used to prepare transition metal doped ZnO such as chemical vapour deposition(CVD), pulsed laser deposition(PLD) and sol gel process, The sol-gel process presents some noticeable advantages, such as; a wide possibility of varying the material properties by changing the composition of the starting solution [1,14], easy to obtain nanoscale materials in volume of gram and its low cost. In the present work, sol- gel spin coating process was used to deposit Ni-doped ZnO films on glass substrate. The variation in structural, optical and electrical properties of Ni doped ZnO film with change in Ni doping concentration has been investigated.

II. EXPERIMENTAL METHOD

Ni²⁺ doping (1,2 and 3 wt%) with ZnO was achieved by dissolving nickel acetate tetrahydrate (Ni(CH₃COO)₂·4H₂O) (in wt%) in a mixture of zinc acetate dihydrate (Zn(CH₃COO)₂·2H₂O) and 2-methoxyethanol. The monoethanolamine(MEA) was added as a stabilizer and the solution was mixed together in a round-bottom flask by stirring at room temperature for 15 minute. The obtained clear solution was heated at 60°C upon magnetic stirring for 60 minute and left undisturbed for 12 hours. The clear and homogenous solution obtained was used as the coating solution for film preparation. The Ni doped ZnO thin film was coated by sol-gel spin coating method at 4000rpm spin rate for 30 seconds by using a spin coater on glass substrate. The film was prepared with 7 coatings with drying at 300°C for 15 minute after each coating. Finally the film on the glass substrate was annealed at 500°C for 60 minute in order to obtain the Ni doped ZnO thin films. In this method three ZnO:Ni samples were prepared by varying nickel acetate tetrahydrate concentration as 1 wt%,2 wt% and 3 wt%.

III. RESULTS AND DISCUSSION

A. X-ray Diffraction Study

Figure 1 shows the XRD patterns of undoped ZnO and Ni doped ZnO thin films. From Figure 1 it can be seen that all the films are polycrystalline in nature and have a preferential c-axis orientation along the (002) direction. The intensity of the (002) peak of the 1 wt% Ni doped ZnO film is very low compared to the undoped sample and the (002) peak intensity increases with increase in Ni doping concentration as 2wt% and 3wt%.

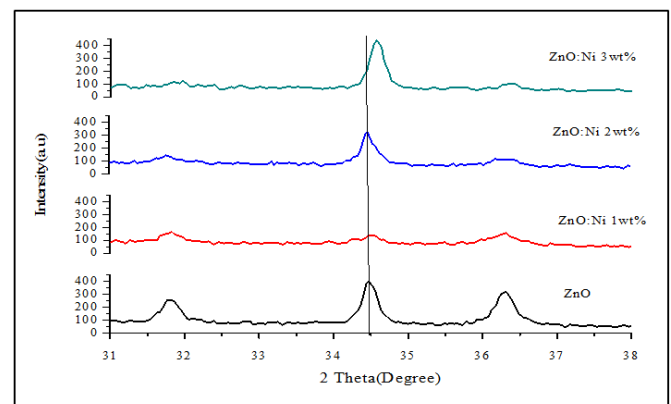


Fig 1:- XRD pattern of ZnO and Ni doped ZnO thin films

There is a slight shift in the position of (002) peak towards the higher angle i.e.from 34.469° for the undoped ZnO to 34.568° for 3wt% Ni doped ZnO film.This slight peak shift may be due to the replacement of zinc ions of the host matrix by Ni ions creating lattice strain and consequently modifying the lattice parameters. The grain size of these films was estimated using the Debye-Scherrer’s formula.

$$D = \frac{k\lambda}{\beta \cos\theta} \tag{1}$$

where D is the grain size of crystallite, k(=0.9) shape factor for spherical particle, λ(=1.54059Å) is the wavelength of X-ray used, β is the broadening of diffraction line measured at half its maximum intensity in radians and θ is the angle of diffraction.

The 2θ position of (002) peak, FWHM and grain size values of ZnO and ZnO:Ni thin films are shown in Table 1. It shows that the grain size increases with the Ni concentration [15,16]. The broadening in X-ray peak is observed with addition of Ni and it indicates the role of nickel in deteriorating the ZnO crystalline quality, which is due to the variance in ionic radii between Zn and Ni[14]. The lattice

constants of the ZnO crystallites were calculated from the prominent peak by using the equation,

$$\frac{1}{d_{hkl}^2} = \frac{4(h^2+hk+k^2)}{3a^2} + \frac{l^2}{c^2} \tag{2}$$

where h, k, l represent the lattice planes and d is the interplanar distance. The stress and strain values of the ZnO films were calculated by using the values of lattice spacing obtained from XRD results, by the formula

$$\text{Stress, } \sigma = -233 \times 10^9 \varepsilon^{hkl} \tag{3}$$

where $\varepsilon^{hkl} = \frac{(d^{hkl} - d_0^{hkl})}{d_0^{hkl}}$ is the elastic strain of the (hkl) planes, d_0^{hkl} is the strain free lattice spacing of the (hkl) lattice plane and d^{hkl} is the lattice spacing of the (hkl) plane of the film[14]. The lattice constants and the estimated stress values are shown in Table 2.

ZnO film on glass	2 Theta(Deg)	FWHM(Deg)	Grain size(nm)
ZnO	34.4697	0.1412	62
ZnO:Ni (1wt%)	34.5357	0.2002	42
ZnO:Ni (2wt%)	34.4691	0.1908	44
ZnO:Ni (3wt%)	34.5687	0.1806	46

Table 1:- Position of (002) peak, FWHM and grain size values of ZnO and Ni doped ZnO thin films on glass substrates

ZnO film on Glass	a Å	c Å	Strain	Stress (*10 ⁹ pa)
ZnO	3.2389	5.1900	-0.00325	0.75725
ZnO:Ni (1wt%)	3.2825	5.2539	-0.00100	0.23260
ZnO:Ni (2wt%)	3.2990	5.2560	-0.00077	0.17902
ZnO:Ni (3wt%)	3.2805	5.2555	-0.00021	0.04562

Table 2:- The lattice constants, strain and stress values of ZnO and Ni doped ZnO thin films on glass substrates

B. UV-Visible Spectroscopic Study

The ZnO and Ni doped ZnO thin films were optically characterized through UV-Visible transmittance spectral curve obtained in the wavelength region from 300 nm to 800 nm. The absorbance spectra and transmittance spectra of the ZnO and Ni doped ZnO thin films for the wavelength range from 300 to 800 nm are presented in Figures 2 and 3 respectively.

The transmittance of the undoped ZnO film was about 95% in the range 400 nm to 800 nm and found to be constant

throughout the visible region (Figure 3). With increase in Ni doping the transmittance found to decrease at lower wavelength portion of the visible region(~ 380 nm to 450 nm) and it lies around 85% at the higher wavelength range of the visible region for all the Ni doped ZnO films.

From the UV-Vis transmittance spectra it is also observed that all the samples have sharp absorption edges in the wavelength region between 350 and 400 nm. The absorption edge found to shift towards the higher wavelength side with increase in Ni doping and this red shift is an

indication of the effect of Ni doping on ZnO. The bandgap values were also determined from the absorbance spectra of ZnO and Ni doped ZnO films, by drawing $(\alpha h\nu)^2$ vs $h\nu$ plots (Tauc's plots). Figures 4 and 5 show the Tauc's plots for ZnO and Ni doped ZnO thin films. The obtained bandgap values (E_g) of the ZnO:Ni(1wt%), ZnO:Ni(2wt%) and ZnO:Ni(3wt%) films from the Tauc's plots are 3.25 eV, 3.24 eV and 3.22 eV respectively. It can be seen that the value of E_g decreases with increase in Ni concentration.

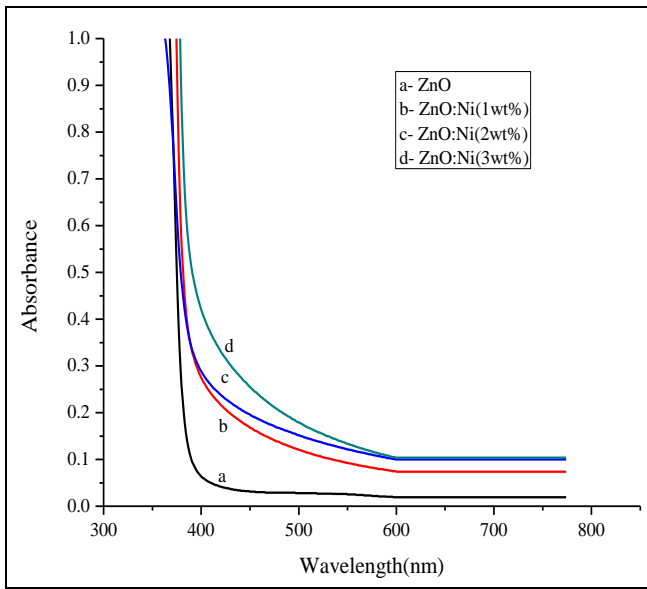


Fig 2:- Absorbance spectra of ZnO and Ni doped ZnO thin films

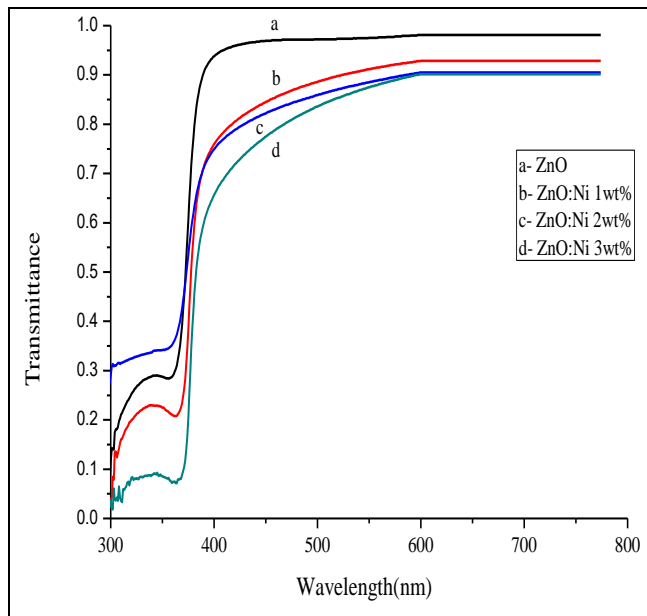


Fig 3:- Transmittance spectra of ZnO and Ni doped ZnO thin films

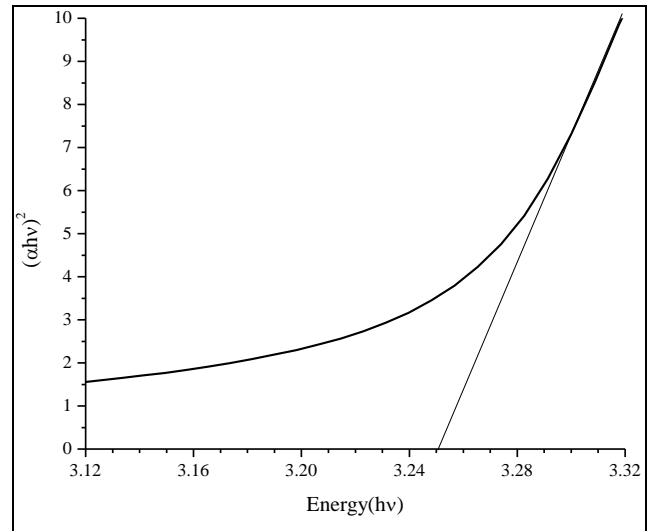


Fig 4:- Tauc's plot of ZnO thin film

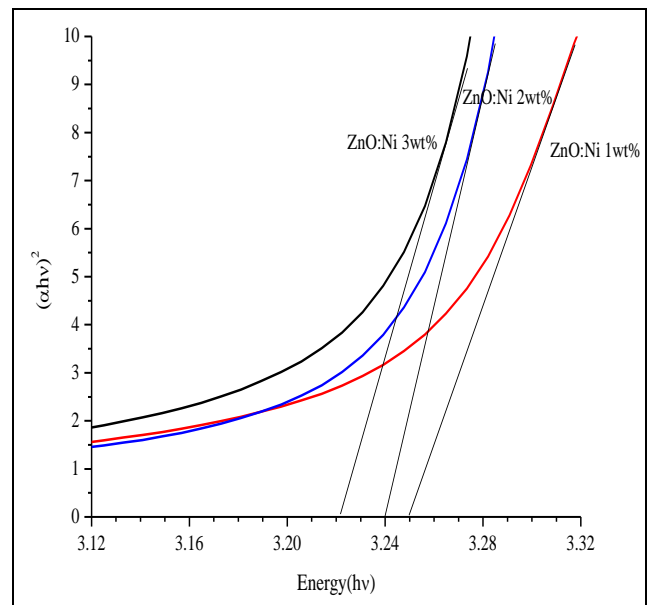


Fig 5:- Tauc's plot of Ni doped ZnO thin films

➤ *Refractive Index Values of Ni doped ZnO thin films*

The Figure 6 shows the optical reflectance spectra of the ZnO and Ni doped ZnO thin films for the range of 300 nm to 800 nm. It is evident that all the films have low reflectance.[17,18]. This low reflectance makes ZnO thin film as an important material for anti-reflection coating. The reflectance of the films found to decrease with increase in Ni doping concentration.

The refractive index of the films can be obtained from the reflectance data using the formula [21],

$$n = \frac{(1+R)}{(1-R)} + \frac{4R}{(1-R)^2} - k^2 \tag{4}$$

where R is the value of reflectance and k is the extinction coefficient which can be derived from the UV-Vis absorbance spectral data using the formula

$$k = \frac{\alpha \lambda}{4\pi} \tag{5}$$

The refractive index values of ZnO and Ni doped ZnO films obtained are plotted in Figure 7.

Figure 7 shows a plot of refractive index (n) versus wavelength (λ) of ZnO thin film and Ni doped ZnO thin films. It can be noted from Figure 7 that all the films have higher refractive index values and these high value of refractive index possessed by ZnO and Ni doped ZnO films make them suitable for antireflection coatings. The refractive index (n) of the films decreases with increase in wavelength and the higher refractive index value lies near the lower visible wavelength region. The value of refractive index decreases with increase in Ni concentration also [15,19].

➤ Dielectric constant values of Ni doped ZnO films

The complex dielectric constant ε(ω) is given by, ε(ω) = ε_r(ω) – iε_i(ω). The real (ε_r) and imaginary (ε_i) parts of dielectric constant can be determined by the relations [20].

$$\begin{aligned} \epsilon_r &= n^2 - k^2 \\ \epsilon_i &= 2nk \end{aligned} \tag{6}$$

Thus if the refractive index and extinction coefficient are known, the real and imaginary parts of dielectric constant of the films can be estimated. The calculated ε_r and ε_i values were plotted against energy (hν) and are shown in Figures 8 and 9 respectively.

The plot versus ε_r and hν shows that the ε_r value is higher for ZnO film compared to Ni doped ZnO films and the value of ε_r increases with increase in hν. Also the value of ε_r for a particular energy decreases with increase in Ni doping in ZnO films. In the plot of ε_i vs hν it could be observed that the ε_i value decreases with increase in the energy hν and the value of ε_i is higher for ZnO film compared with Ni doped ZnO films.

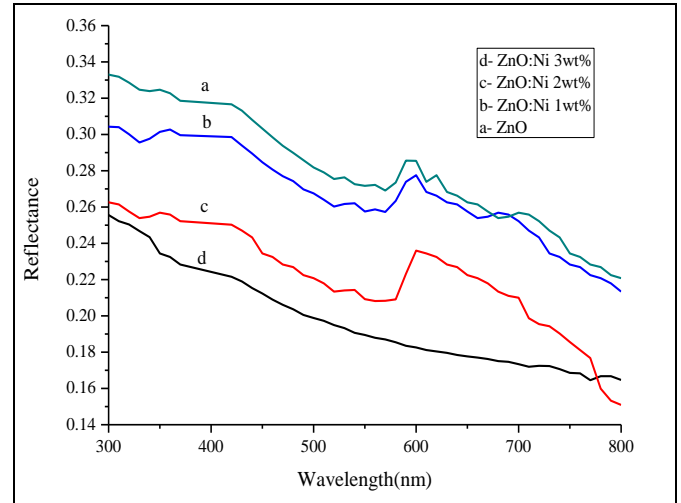


Fig 6:- Reflectance spectra of undoped and Ni doped ZnO thin films

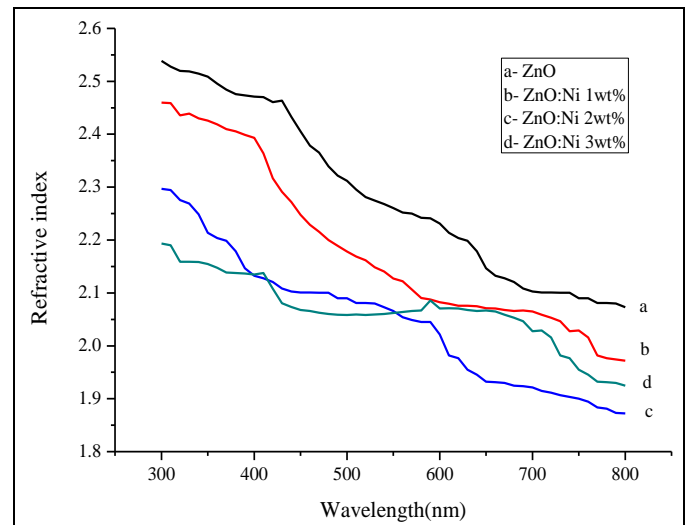


Fig 7:- Refractive index n(λ) of ZnO and Ni doped ZnO thin films

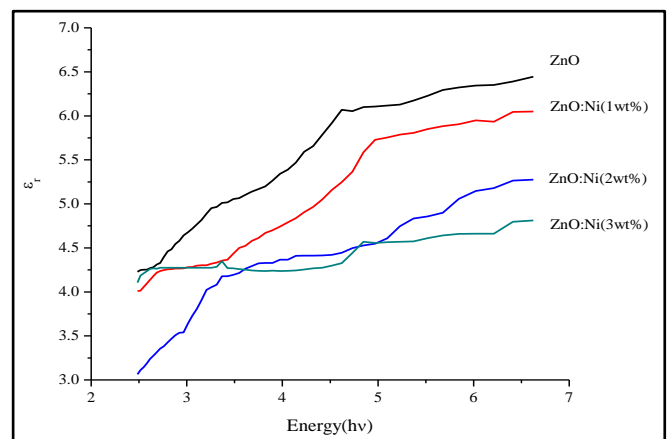


Fig 8: Variation of real part of dielectric constant as a function of photon energy of ZnO and Ni doped ZnO thin films

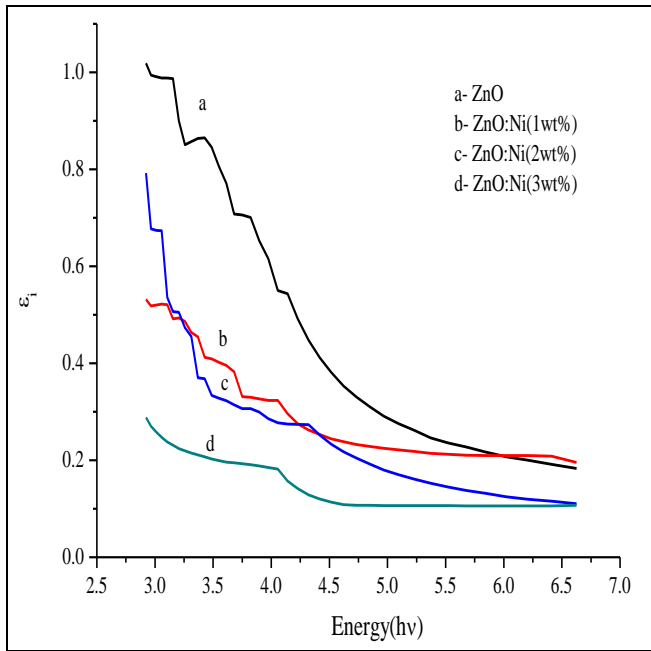


Fig 9: Variation of imaginary part of dielectric constant as a function of photon energy of ZnO and Ni doped ZnO thin films

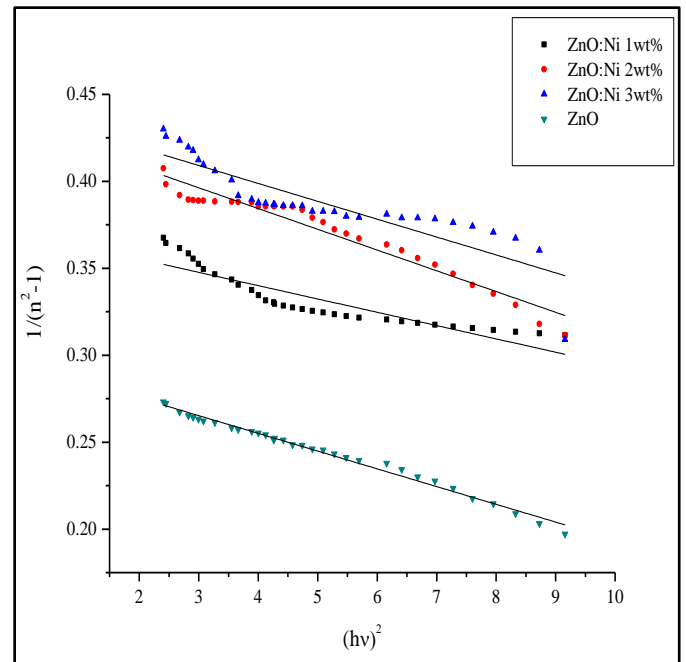


Fig 10: Plots of 1/(n²-1) verses energy for ZnO and Ni doped ZnO thin films

➤ *Single oscillator model for ZnO films*

A single-oscillator model proposed by S.H.Wemple and M. Di Domenico for thin films was helpful to reveal the unknown and hidden information on the optical origin. According to this model, the optical data can be described to an excellent approximation by the relation.

$$n^2 - 1 = \frac{E_d E_0}{E_0^2 - E^2} \tag{7}$$

where, E(=hv) is the photon energy, n is the refractive index, E₀ is the single-effective oscillator energy and E_d is the dispersion energy which is a measure of the average strength of the inter band optical transitions. Plotting 1/(n²-1) against (hv)² can yield the oscillator parameters by fitting a straight line. Figure 10 shows the plot of 1/(n²-1) vs (hv)² for the Ni doped ZnO thin films. The values of E₀ and E_d can be determined directly from the slope (E₀E_d)⁻¹ and the intercept on the vertical axis, (E₀/E_d). The calculated values of E₀ and E_d are listed in Table 3. In addition, the optical band gap (E_g) can also be obtained using the relation E_g=E₀/2 [19]. The optical band gap values (E_g) of the undoped ZnO and 1wt%, 2wt% and 3wt% Ni doped ZnO thin films were calculated using this relation are also given in Table 3. The E_g value obtained by this model for undoped ZnO film exactly matches with that value derived from the Tauc's plot. The E_g values of Ni doped ZnO films obtained from Tauc's plot and single oscillator model are also found to have tolerable difference. Similar result was obtained by Bakr et. al, [20] also.

	E ₀ (eV)	E _d (eV)	E _g (eV)	E _g value obtained from Tauc's plot(eV)
Undoped ZnO	6.50	16.90	3.25	3.25
ZnO:Ni 1%	6.30	15.84	3.15	3.25
ZnO:Ni 2%	6.13	16.31	3.07	3.24
ZnO:Ni 3%	6.06	20.40	3.03	3.22

Table 3:- Calculated E_d and E₀ values for ZnO and Ni doped ZnO thin films

C. *Photoluminescence Study*

Figure 11 shows the PL spectra of the ZnO and nickel doped ZnO thin films coated on glass substrates. Two sharp visible emission peaks centered at 414 and 489 nm are appearing in the spectra of Ni doped ZnO thin films. It is very interesting to note that the peaks corresponding to violet (414 nm) and blue-green (489 nm) emission increases along with increase in Ni doping concentration. The violet emission peak at 414 nm might be due to structural and surface defects, such as oxygen vacancies and zinc interstitials on the surface of the thin films. The 489 nm peak is absent for undoped ZnO film. So the origin of blue-green luminescence peak at 489 nm can be related to the defect levels introduced due to substitution of Ni²⁺ ions in the Zn²⁺ sites by doping.

This result is in conformity with the result obtained by Gayen et. al,[21].

D. Four Point Probe Measurement Study

Figure 12 shows the comparison plot of V-I characteristic curves of Ni doped ZnO thin films on glass substrate. The V-I characteristic curve of Ni doped ZnO thin films show that for all the samples the current increases with increase in voltage.

The resistivity values obtained from the V-I plots for various ZnO:Ni films on glass are given in Table 4. From Table 4 it can be observed that the resistivity values obtained from V-I characteristic curves of Ni doped ZnO films decreases with increase in Ni doping concentration. The resistivity value of the undoped ZnO film on glass substrate was 1.3 Ωcm. This falls drastically to 0.25 Ωcm with 1wt% Ni doping and still goes down to 0.19 Ωcm and 0.09 Ωcm as the Ni doping concentration increases as 2wt% and 3wt% respectively. This reduction in resistivity on Ni doping may be due to the enhancement in the itinerant electron concentration caused by the replacement of Zn²⁺ by Ni²⁺ ions on doping.

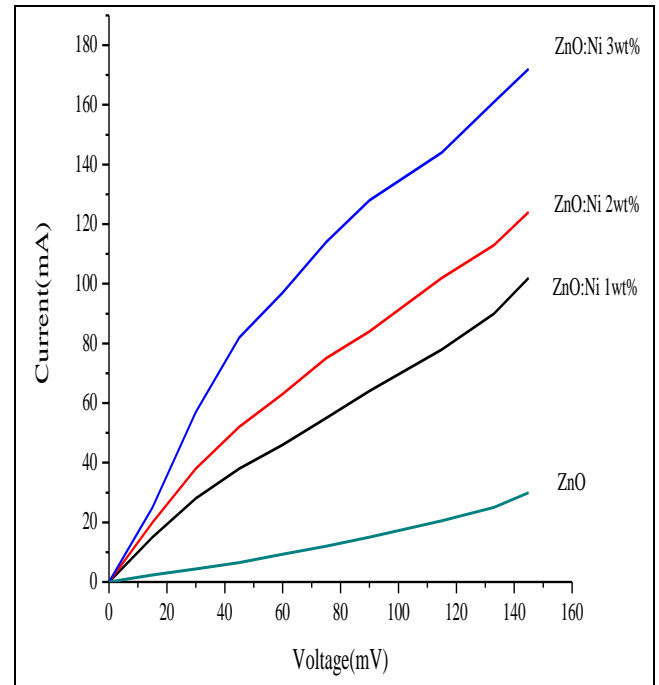


Fig 12: V-I characteristic curves of undoped ZnO and Ni doped ZnO thin films on glass substrate

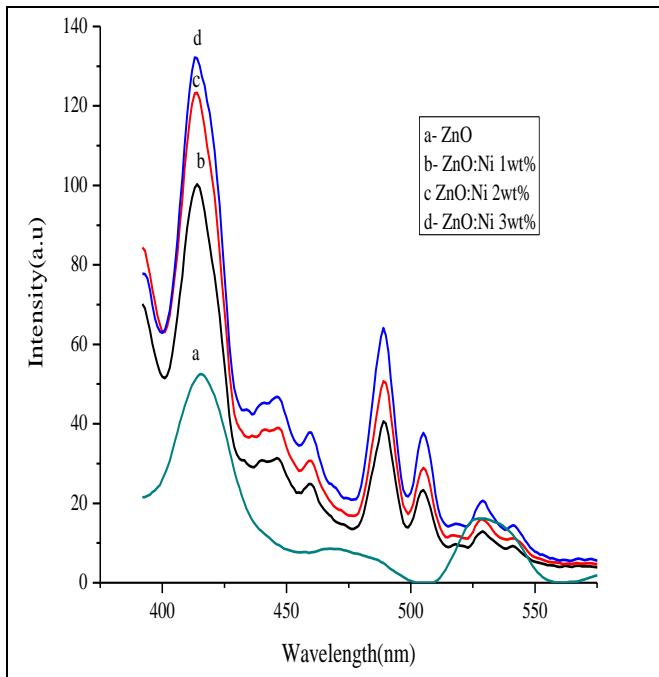


Fig 11: Photoluminescence peaks for ZnO and Ni doped ZnO thin films

Concentration of Ni	Resistivity(Ω cm)
Undoped ZnO	1.3
1 wt%	0.25
2wt%	0.19
3wt%	0.09

Table 4:Resistivity variation of Ni doped ZnO thin films on glass substrates

IV. CONCLUSION

All the films are polycrystalline in nature and have a preferential c-axis orientation along the (002) direction. There is a slight shift in the position of (002) peak towards the higher angle i.e. from 34.469° for the undoped ZnO to 34.568° for 3wt% Ni doped ZnO film. The low reflectance of ZnO and Ni doped ZnO thin films makes ZnO thin film as an important material for anti-reflection coating. The E_g values of Ni doped ZnO films obtained from Tauc’s plot and single oscillator model are also found to have tolerable difference. The violet photoluminescence at room temperature shows a possibility of application in organic photoluminescence devices. The resistivity values of Ni doped ZnO films decreases with increase in Ni doping concentration.

REFERENCES

- [1]. N. V. Kaneva and C. D. Dushkin, *Bulg. Chem. Comm.* 43, 259(2011)
- [2]. D. Song, A.G. Aberle and J. Xia, *Appl. Surf. Sci.*195,291(2002)
- [3]. A. Miyake, H. Kominami, H. Tatsuoka, H. Kuwabara, Y. Nakanishi and Y. Hatanaka, *J.Cryst.Growth* 215, 294(2000)
- [4]. N.V.Russell, A.V.Chadwick and .Wilson, *Nuc.l.Instrum.Methods.Phys.Res.B*.97,575 (1995)
- [5]. M.A. Martinez, J. Herrero and M.T. Gutierrez, *Sol. Energy Mater.Sol.Cells* 45, 75(1997)
- [6]. R. Elilarassi and G. Chandrasekaran, *Am.J.Mater.Sci.* 2,46(2012)
- [7]. V. Musat, B. Teixeira, E. Fortunato, R.C.C. Monteiro and P.Vilarinho, *Surf. Coat.Technol.*180,659(2004)
- [8]. V. Gokulkrishnan, V. Purushothaman, E.Arthi, K.Jeganathan and K. Ramamurthi, *Phys. Status Solidi A* 209, 1481(2012)
- [9]. Y. Z Peng, T. Liew, W. D. Song, C. W. An, K.L.Teo and T. C. Chong, *J Supercond Nov Mag.*18,97(2005)
- [10]. J. A.Najim and J. M. Rozaiq, *Int. Lett.Chem. Phys. Astro.* 10, 137(2013)
- [11]. K. Huang, Z. Tang, L. Zhang, J. Yu, J.Lv, X.Liu and F.Liu, *Appl.Surface.Sci.* 258, 3710(2012)
- [12]. J. Mohapatra, D.K.Mishra, S. K. Kamilla, V. R. R. Medicherla, D. M. Phase, V.Bermaand and S. K Singh, *Phys. Status Solidi B* 248,1352(2011)
- [13]. M. Rajendraprasad Reddy, V. Supriya, M. Sugiyama and K. T. Ramakrishna Reddy, *Conference Papers in Energy*,2013,1 (2013)Article ID 508170
- [14]. G. J. Huang, J. B. Wang, X. L Zhong, G. C. Zhou, H. L. Yan, *J Mater Sci.* 42, 6464(2007)
- [15]. A.Mhamdi, B.Ouni, A.Amlouk, K.Boubaker, M. Amlouk, *J. Alloys Compd.* 582,810(2014)
- [16]. T. K. Pathak, P. Singh and L. P. Purohit, *Int. J. Electronics and Electrical Engineering* ISSN : 22772, 31(2012)
- [17]. M.Caglar, Y.Caglar, S.Ilican, *J. Optoelectron Adv Mater.* 8, 1410 (2006)
- [18]. I. A. Ezenwa, *Res. J. Chem Sci.* 2, 26 (2012)
- [19]. X. Y. Gao, Y. Liang, Q. G. Lin, *J Korean Phys Soc.* 57, 710 (2010)
- [20]. N. A. Bakr, A. M. Funde, V. S. Waman, M. M. Kamble, R. R. Hawaldar, D. P. Amalnerkar, S. W. Gosavi and S. R. Jadkar, *Pramana* 76, 519 (2011)
- [21]. R.N. Gayen, A.Rajaram, R.Bhar and A. K. Pal, *Thin Solid Films* 518, 1627 (2010)